

Supporting Information:

Theoretical investigation of enhancement of positron affinity by vibration and dimerization of non-polar carbon disulfide

Miku Furushima, Daisuke Yoshida, Yukiumi Kita,* Tomomi Shimazaki, and
Masanori Tachikawa*

*Quantum Chemistry Division, Yokohama City University, Seto 22-2, Kanazawa-ku,
Yokohama 236-0027, Kanagawa, Japan*

E-mail: ykita@yokohama-cu.ac.jp; tachi@yokohama-cu.ac.jp

Potential energy curve for C_2S_4

In this work, we first obtained the equilibrium structure of the carbon disulfide dimer C_2S_4 in the CCSD/aug-cc-pVDZ calculation. The calculation method and detailed structure parameters of the the equilibrium geometry can be found in the main paper, while in Figure S2 in the Supporting Information, we show the potential energy curve for C_2S_4 with respect to the CS_2 - CS_2 intermolecular separation R_{CC} . In this calculation, we carried out partial optimizations for all CS internuclear distances in every R_{CC} . We found the electronic interaction energy with respect to the dissociation asymptotic energy to be 2.07 kcal/mol, and zero-point vibrational energies in the harmonic approximation to be 1493 cm^{-1} for CS_2 and 3043 cm^{-1} for C_2S_4 . Thus, we obtained the binding energy as 1.91 kcal/mol.

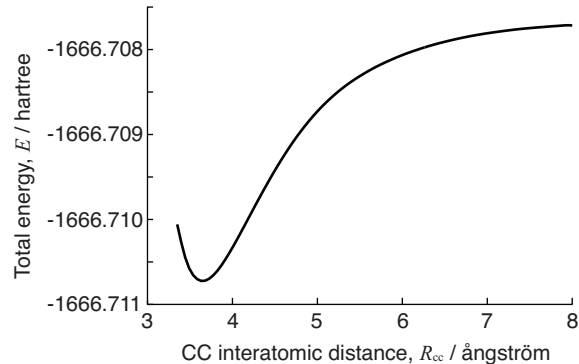


Figure S1: Potential energy curve for the CS₂ dimer with respect to CS₂–CS₂ intermolecular separation.

Normal mode vibrations for C₂S₄

Figure S2 shows schematic representations of twelve normal mode vibrations for C₂S₄ calculated by CCSD/aug-cc-pVDZ method, which are introduced in Table 1 in the main paper. Here, mode numbers i are defined in ascending order of frequencies. The first three normal modes $i = 1-4$; the rotational twisting, the wagging (degenerate), and the intermolecular stretching modes are unique vibrational modes to C₂S₄, where geometries for every CS₂ units do not change. On the other hand, all other normal modes can be found to involve geometrical changes of CS₂ units due to SCS bending and CS stretching.

For the CS₂ monomer, the same calculation level provides vibrational frequencies of 382, 675, and 1540 cm⁻¹ for the symmetric bending, symmetric stretching, and asymmetric stretching modes in the harmonic approximation. We found that due to formation of the dimer, vibrational frequencies of only the SCS bending modes ($i = 5-8$) slightly decrease, while those of both symmetric and asymmetric stretching modes ($i = 9-12$) do not change. In the C₂S₄ system, symmetric π type molecular orbitals as well as antisymmetric ones of two CS₂ units make finite orbital overlaps, and contribute into the intermolecular bonding. This effect can be considered to make π type bond stiffness of a CS₂ unit slightly weak, and results in decreasing the vibrational energies for the SCS bending modes rather.

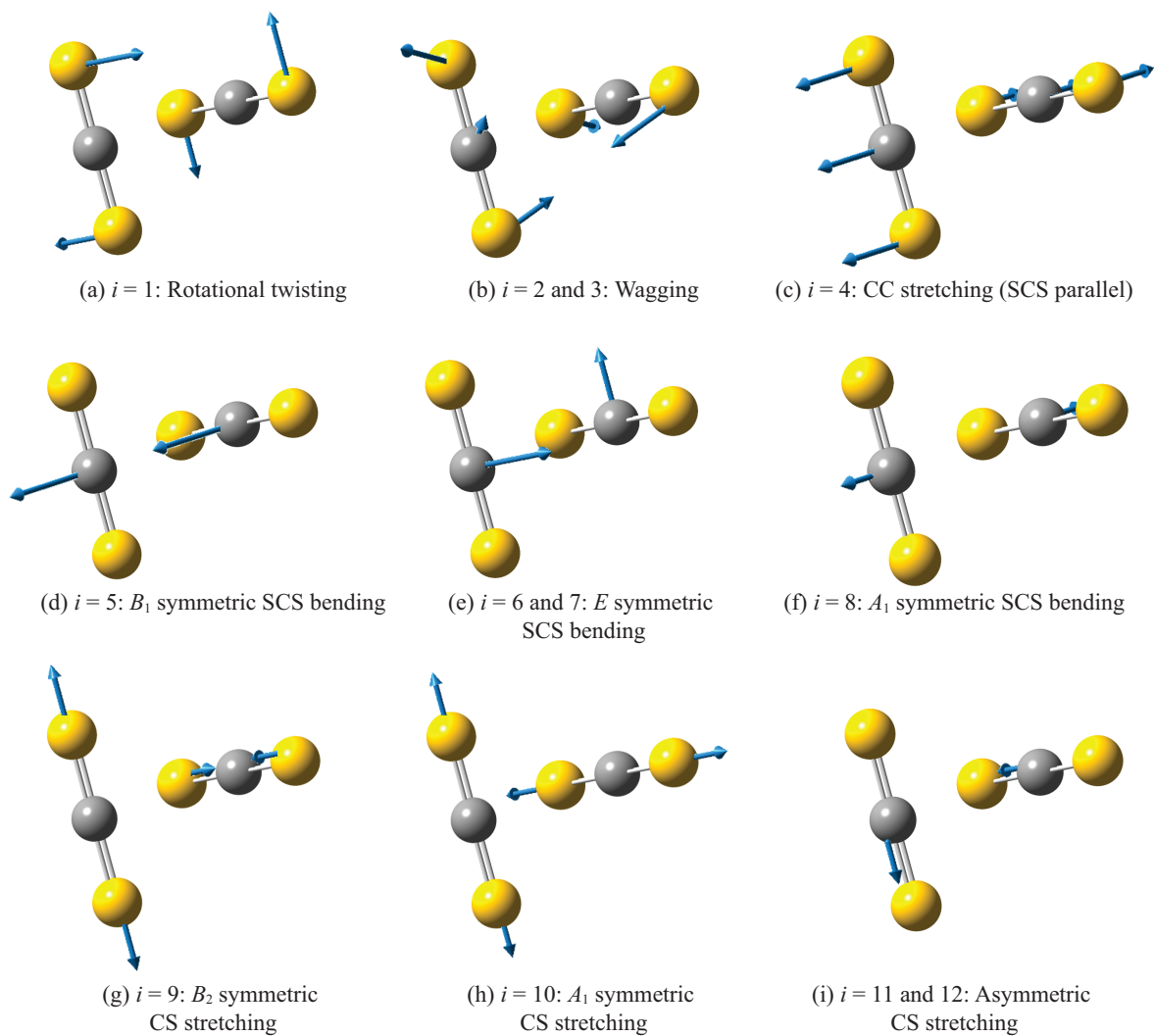


Figure S2: Schematic representations of normal mode vibrations for C_2S_4 . Carbon and sulfur atoms are shown by gray and yellow balls, respectively.

Supplemental data for vibrational averaged PA for C₂S₄

In the main paper, we mainly classified vibrational effects of the ground state vibrational modes $n_i = 0$ on the positron affinity (PA) into three schemes; in compared to $\text{PA}(\mathbf{Q}_{\text{eq}}) = 46.18$ meV for the equilibrium geometry, (A) vibrational averaged positron affinity PA_{ν_i} over the ground vibrational modes of $\psi_{\nu_i}(Q_i)$, decreased or almost unchanged, (B) PA_{ν_i} increased by increase of α_{ν_i} , and (C) PA_{ν_i} increased by increase of μ_{ν_i} . We show detailed information of vibrational averaged quantities for PA, μ , and α of all the ground state vibrational modes in Table S1, where for an arbitrary physical quantity $A(Q_i)$ as a function of the i -th normal mode coordinate Q_i , the vibrational contribution ΔA_{ν_i} was defined by

$$\Delta A_{\nu_i} = \frac{\int A(Q_i) |\psi_{\nu_i}(Q_i)|^2 dQ_i}{\int |\psi_{\nu_i}(Q_i)|^2 dQ_i} - A(\mathbf{Q}_{\text{eq}}). \quad (1)$$

Along with the vibrational averaged values, we also show PA, μ , and α as functions of Q_i for the normal modes i except for $i = 4, 8, 11$ and 12 discussed in the main paper. For the A_1 symmetric stretching mode $i = 10$ with the IR inactive, PA and α change almost linearly with the displacement Q_{10} , as shown in Figure S3 (e). $\text{PA}_{\nu_{10}} = 46.12$ meV is slightly decreased in compared to $\text{PA}(\mathbf{Q}_{\text{eq}}) = 46.18$ meV at the equilibrium geometry as shown in Table S1. Thus, this mode is similar to the mode $i = 4$ introduced in the main paper, which was classified as the scheme (A) above.

For the rotational twisting mode $i = 1$ with the IR inactive, PA_{ν_1} can be found to be increased by 0.11 meV in compared to $\text{PA}(\mathbf{Q}_{\text{eq}})$, where the vertical PA increases as α increases, as shown in Figure S3 (d). This mode exhibits the same characteristics to the mode $i = 8$ classified as the scheme (B) in the main paper.

In contrast, the B_1 symmetric SCS bending mode $i = 5$ and the E symmetric SCS bending ones $i = 6$ and 7 exhibit a similar tendency that the vertical PA increases as μ increases, as shown in Figure S3 (b)-(c), and consequently, both PA_{ν_5} and $\text{PA}_{\nu_{6,7}}$ for the ground state vibrational modes are increased by 0.14 and 0.26 meV, respectively. This is

also the same effect to the modes $i = 11$ and 12 as scheme (C), discussed in the main paper.

On the other hand, only for the degenerate wagging modes $i = 2$ and 3 , exceptionally, these μ_{ν_i} are slightly increased, whereas PA_{ν_i} are decreased due to a negative correlation between PA and μ as shown in Figure S3 (a). Although there are a few vibrational modes to decrease or not to affect on the vibrational averaged PA, great contributions from the other vibrational modes of schemes (A) and (B) yield the enhancement of the vibrational averaged PA for C_2S_4 .

Table S1: Vibrational contribution of positron affinity, dipole moment and dipole polarizability for each ground state normal mode.

Normal mode i	Infrared active(A)/inactive(I)	ΔPA_{ν_i} (meV)	$\Delta\mu_{\nu_i}$ (debye)	$\Delta\alpha_{\nu_i}$ (bohr ³)
1	I	0.11	0	0.2
2, 3	A	-0.04	0.008	0.1
4	I	-9.22	0	0.8
5	A	0.14	0.019	0.1
6, 7	A	0.26	0.024	0.1
8	I	0.15	0	0.1
9	I ^a	0.00	0.001	0.1
10	I	-0.06	0	0.0
11, 12	A	3.97	0.458	0.0

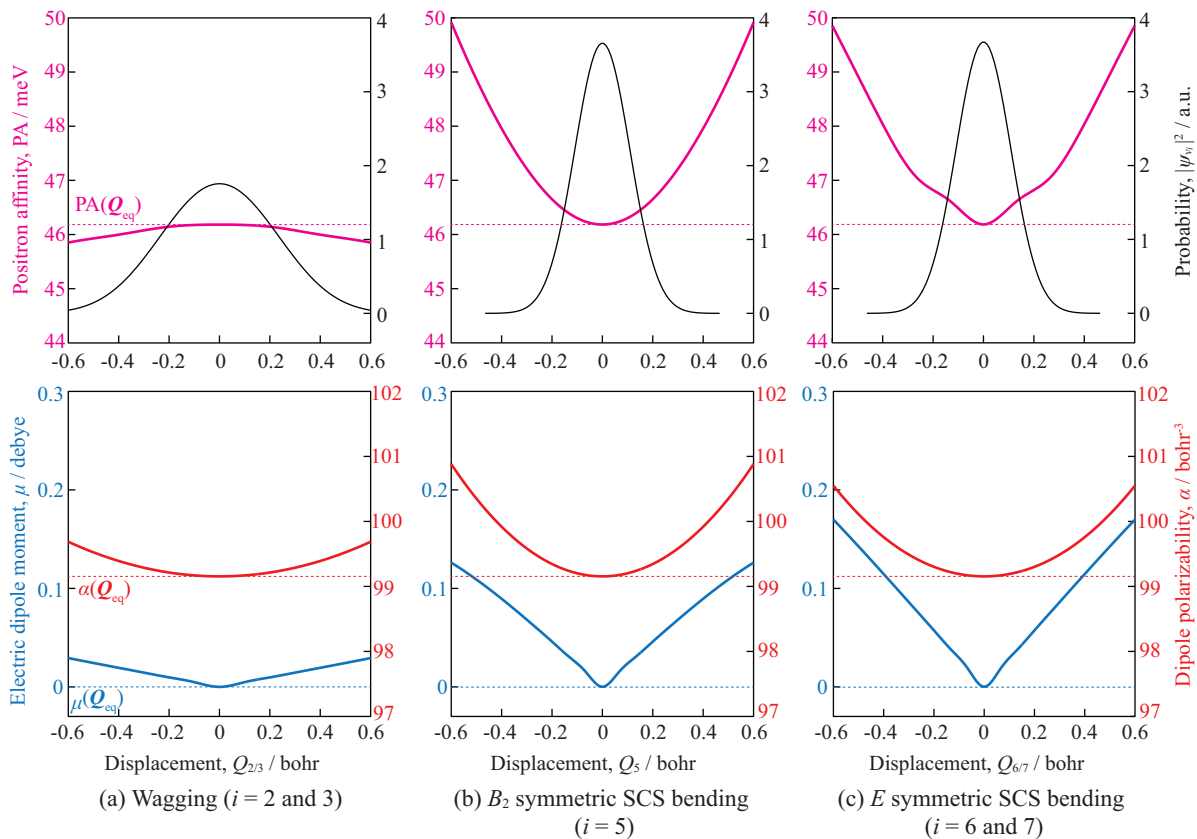


Figure S3: Positron affinity PA, dipole moment μ , and dipole polarizability α as functions of the normal mode vibrational coordinates for IR active modes $i = 2, 3, 5, 6,$ and $7,$ and IR inactive modes $i = 1, 9,$ and $10.$

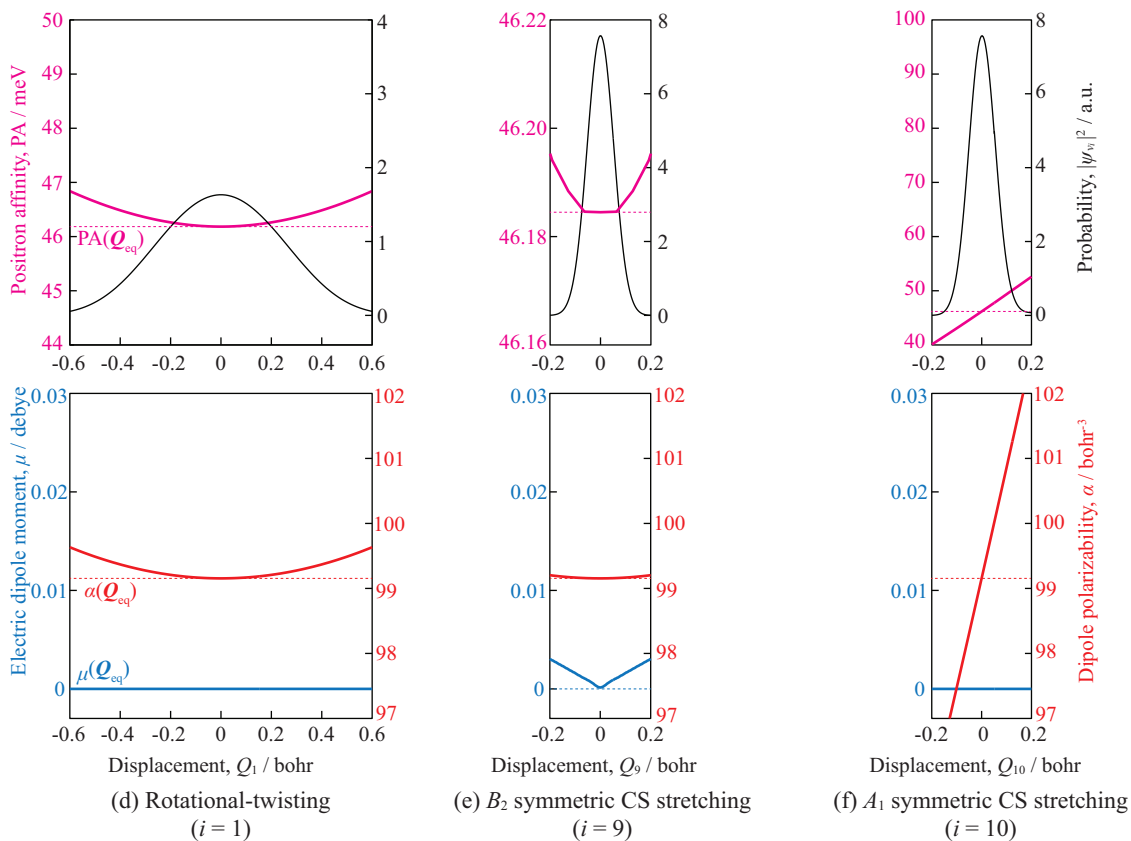


Figure S3: (Continued) Positron affinity PA, dipole moment μ , and dipole polarizability α as functions of the normal mode vibrational coordinates for IR active modes $i = 2, 3, 5, 6,$ and $7,$ and IR inactive modes $i = 1, 9,$ and $10.$

Vibrational wave functions for the excited vibrational states

In the main paper, we obtained reasonable positron kinetic energies K_ν by considering the vibrational averaged PA for some excited vibrational states. In Figure S4, we show two-dimensional vibrational wave functions for the excited vibrational states, $(n_1, n_9, n_{10}, n_{11}, n_{12}) = (0, 1, 1, 0, 0)$, $(0, 2, 0, 0, 0)$, $(0, 0, 2, 0, 0)$, $(0, 0, 0, 0, 1)$, and $(1, 0, 0, 0, 1)$, discussed in the main paper, where all the other vibrational quantum numbers, n_i ($i = 2-8$) are zeros. The excited vibrational wave functions for (n_i, n_j) are separated by wave function nodes corresponding to ν_i and ν_j .

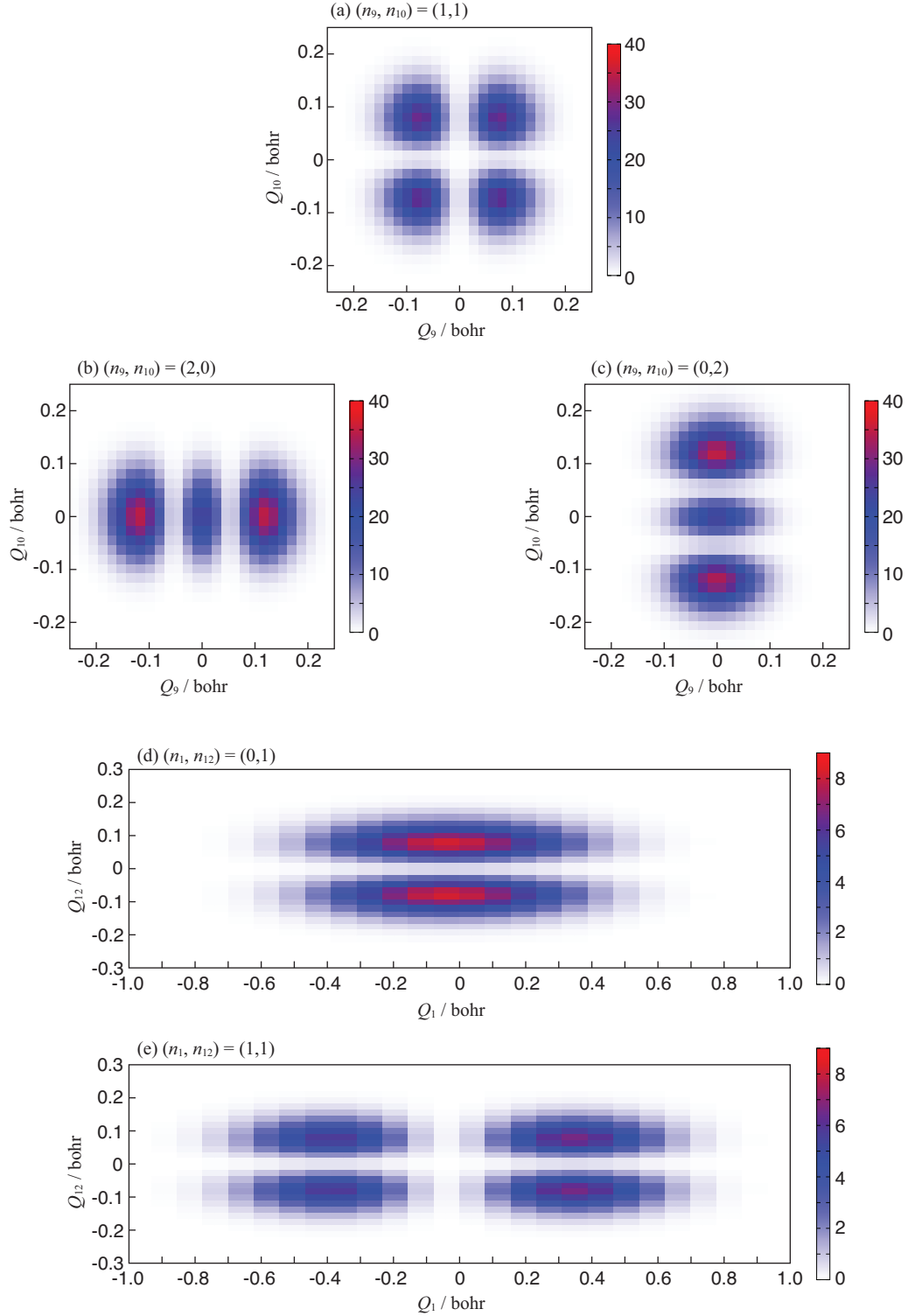


Figure S4: Two-dimensional vibrational wave functions for the vibrational excited states discussed in the main paper; (a) $(n_9, n_{10}) = (1, 1)$, (b) $(n_9, n_{10}) = (2, 0)$, (c) $(n_9, n_{10}) = (0, 2)$, (d) $(n_1, n_{12}) = (0, 1)$, and (e) $(n_1, n_{12}) = (1, 1)$, where all omitted vibrational modes are the ground level ($n_i = 0$). In (a)-(e), the probability density $|\Psi_\nu|^2$ are shown in units of a.u., and displacements Q_i are shown in units of bohr.